Volume 11 Number 18 1983 Nucleic Acids Research

Similar binding of the carcinostatic drugs *cis*-$[Pt(NH_3)_2Cl_2]$ and $[Ru(NH_3)_5Cl]$ Cl_2 to $tRNA^{phe}$ and a comparison with the binding of the inactive *trans*-$[Pt(NH_3)_2Cl_2]$ complex – reluctance in binding to Watson-Crick base pairs within double helix

John R.Rubin, Michal Sabat* and Muttaiya Sundaralingam

Department of Biochemistry, College of Agricultural and Life Sciences, University of Wisconsin-Madison, Madison, WI 53706, USA

Received 6 May 1983; Revised and Accepted 22 August 1983

ABSTRACT

A comparative study of the binding of square planar cis- and trans-$[Pt(NH_3)_2Cl_2]$ complexes and the octahedral $[Ru(NH_3)_5(H_2O)]^{3+}$ complex to $tRNA^{phe}$ from yeast was carried out by X-ray crystallography. Both of the carcinostatic compounds, cis-$[Pt(NH_3)_2Cl_2]$ and $[Ru(NH_3)_5(H_2O)]^{3+}$ show similarities in their mode of binding to tRNA. These complexes bind specifically to the N(7) positions of guanines G15 and G18 in the dihydrouridine loop. $[Ru(NH_3)_5(H_2O)]^{3+}$ has an additional binding site at N(7) of residue G1 after extensive soaking times (58 days). A noncovalent binding site for ruthenium is also observed in the deep groove of the acceptor stem helix with shorter (25 days) soaking time. The major binding site for the inactive trans-$[Pt(NH_3)Cl_2]$ complex is at the N(1) position of residue A73, with minor trans-Pt binding sites at the N(7) positions of residues G^m34, G18 and G43. The similarities in the binding modes of cis-$[Pt(NH_3)_2Cl_2]$ and $[Ru(NH_3)_5(H_2O)]^{3+}$ are expected to be related to their carcinostatic properties.

INTRODUCTION

Since the initial discovery that cis-$[Pt(NH_3)_2Cl_2]$ (cis-Pt) is a potent anticancer agent (1) much research has been undertaken to elucidate the mechanism of action of this drug. It is generally accepted that the anticancer activity of the cis-platinates results from their interactions with tumor cell DNA (2). Furthermore, solution studies have shown that the guanine bases of DNA are selectively attacked at low drug to DNA ratios (3). In contrast to the cis-platinum compounds, the trans-isomers are inactive against tumor cells (4). This suggests that the two labile chloride ligands must be cis to one another for the platinum complex to be active. This requirement has led some researchers to predict that cis-platinum may form intra-strand

crosslinks between adjacent guanines on the DNA chain (5). Support for this mode of complexation has come from solution studies on polynucleotides (6) as well as single crystal X-ray diffraction studies of cis-platinum complexes with nucleic acid constituents (7-10). Alternatively, it has been proposed that cis-platinum forms bidentate complexes to the N(7) and O(6) sites of DNA guanines (4).

The successful application of the square planar cis-$[Pt(NH_3)_2Cl_2]$ as an anticancer drug (1) has stimulated research on other potentially oncostatic metal complexes. The octahedral ammine ruthenium complex $[Ru(NH_3)_5(H_2O)]^{3+}$ is an effective inhibitor of cellular DNA synthesis (11). In vitro studies of the binding of $[Ru(NH_3)_5(H_2O)]^{3+}$ have suggested that the drug binds specifically to the N(7) position of DNA guanines (12) in a manner similar to that postulated for the interaction of cis-$[Pt(NH_3)_2Cl_2]$ (3,13). In order to gain some insights into the mechanism of action of cis- platinum and ruthenium pentaammine drugs we have undertaken a comparative crystallographic investigation of their binding, as well as the binding of the inactive trans-$[Pt(NH_3)_2Cl_2]$ complex, to $tRNA^{phe}$.

MATERIALS AND METHODS

Cis-$[Pt(NH_3)_2Cl_2]$ and trans- $[Pt(NH_3)_2Cl_2]$ were generous gifts from Dr. B. Rosenberg, Michigan State University and Dr. D. T. Thompson, Johnson Matthey, U.K., respectively. $[Ru(NH_3)_5Cl]\ Cl_2$ was prepared by refluxing $[Ru(NH_3)_6]Cl_3$ (ICN Pharmaceuticals Inc.) in 6M HCl for four hours followed by crystallization from 0.1M HCl (14). Yeast phenylalanine tRNA was obtained from Boehringer, Mannheim, Ltd. Native crystals of $tRNA^{phe}$ were prepared by batch techniques as described previously (15). Crystals of the platinum-tRNA complexes were prepared by soaking $tRNA^{phe}$ crystals in crystal stabilizing buffer (10mM $MgCl_2$, 10mM sodium cacodylate (pH=6.3), 20% v/v 2-methyl 2,4 pentanediol) saturated in the platinum compound (Table 1). Crystals of the pentaammineruthenium(III)-$tRNA^{phe}$ complex were prepared by soaking native $tRNA^{phe}$ crystals in solutions containing saturated $[Ru(NH_3)_5Cl]Cl_2$ in the same buffer as above. Two different crystals soaked in $[Ru(NH_3)_5Cl]Cl_2$ solution for different lengths of time were examined independently. Crystals Ruphe(25) and Ruphe(58) were soaked for 25 days and 58 days, respectively. Both ruthenium soaked crystals were stained red. Crystals were sealed in thin-walled glass capillaries for X-ray data collection. X-ray diffraction data were collected on an Enraf-Nonius CAD-4 diffractometer using the omega scan mode and a variable scan speed. Crystallographic data for the native

TABLE I. Crystallographic Data

	cis-Pt-tRNA^{phe}	trans-Pt-tRNA^{phe}	Native
Ligand concentration	saturated cis-$Pt(NH_3)_2Cl_2$, 10 mM $MgCl_2$	saturated trans-$Pt(NH_3)_2Cl_2$, 10 mM $MgCl_2$	10 mM $MgCl_2$
Soaking time	10 d.	23 d.	-
Space group	$P2_122_1$	$P2_122_1$	$P2_122_1$
Unit cell (Å)	a=33.18(3) b=55.67(4) c=159.8(1)	a=33.16(3) b=55.82(3) c=159.44(6)	a=33.14(3) b=55.75(2) c=158.80(5)
Resolution (Å)	5.5	5.5	4.0
No. of reflections observed (2σ)	849 (79%)	998 (90%)	2481 (89%)
$\frac{\Sigma \left\|\|F_{Pt}\| - \|F_{Nat}\|\right\|}{\Sigma \|F_{Nat}\|}$	0.27	0.13	-

TABLE II. Ru-tRNA^{phe} Crystallographic Data

	Ruphe(25)	Ruphe(58)	Native
Ligand Concentration	saturated $[Ru(NH_3)_5Cl]Cl_2$ 10 mM $MgCl_2$	same	10 mM $MgCl_2$ 1 mM spermine
Soaking time	25 d	58 d	-
Space Group	$P2_122_1$	$P2_122_1$	$P2_122_1$
Unit Cell Constants(Å)	a=33.14(1) b=55.88(1) c=159.63(4)	a=33.96(3) b=55.41(1) c=158.11(3)	a=33.14(3) b=55.75(2) c=158.80(5)
Resolution(Å)	4.0	4.0	4.0
Observed Reflections	2511 (80%)	1816 (68%)	2481 (89%)
ΔB in scaling	-10.20	4.50	-
$\frac{\Sigma\left\|\left\|F_{Ru}\right\|-\left\|F_{Nat}\right\|\right\|}{\Sigma\left\|F_{Nat}\right\|}$	0.19	0.28	-

and metal complexed crystals are given in Tables I and II. The X-ray diffraction data were corrected for Lorentz and polarization effects and scaled to the native data set in each of eight concentric shells on $\sin\theta/\lambda$. The native tRNA phases (α_{calc}) were calculated from the published tRNA^{phe} atomic coordinates (16). The locations of the platinum and ruthenium binding sites were determined from the difference electron density maps calculated using coefficients of the form $F_{complex} - F_{native}\ \alpha_{calc}$, where $F_{complex}$ and F_{native} are the observed structure factor amplitudes for the metal complexed and native tRNA crystals, respectively.

MOLECULAR MODEL FITTING

The interpretation of the metal coordination sites on the tRNA was facilitated by the use of a Vector General graphics system interfaced to a

PDP/11-35 computer. Since it was not possible to distinguish the ligands on platinum and ruthenium in the low resolution difference electron density maps, the square planar geometry observed in the crystal structure of the $[Pt(NH_3)_2(H_2O)$-(3'-CMP)] complex (17a) was used to fit the difference electron density peaks. The positions of the tRNA bound ruthenium complex ions were determined from the highest residual electron density peaks in the Ru - native difference electron density maps (c.f. figure 6). At 4 Å resolution it was not possible to locate the ammonia ligands on the ruthenium. Instead, the octahedral geometry of the $[Ru(NH_3)_5]^{3+}$ group observed in the $[Ru(NH_3)_5$ (hypoxanthine)] crystal structure (17b) was assumed. The most probable orientation of the complex was deduced from the distribution of tRNA atoms surrounding the $[Ru(NH_3)_5]^{3+}$ peaks with the aid of molecular graphics. The crystallographic calculations and the molecular graphics work were carried out in our laboratory using a PDP/11-35 computer. The necessary programs were written by Drs. S. T. Rao, J. P. McAllister, E. A. Merritt and T. Haromy.

RESULTS

The major metal binding sites are summarized in Tables III and IV.

Cis-Pt tRNA Complex

Crystals soaked in cis-Pt solution for four days showed no evidence of platinum binding to tRNA. Crystals soaked for longer periods of time (10 days) under identical conditions (Table I) showed two strong cis-Pt binding sites (Table III). Both of these platinum sites are located in a segment of the dihydrouridine loop of $tRNA^{phe}$. One platinum is directly coordinated to N(7) of G15 and the ligands on the platinum (NH_3 and H_2O) form hydrogen bonds to phosphate oxygens on P14 and P15, the exocyclic oxygens O(4) of U8 and O(6) of G15 (figure 1). The second $[Pt(NH_3)_2(H_2O)]^{2+}$ complex is coordinated to N(7) of G18 and the water ligand forms interligand hydrogen bonds to N(6) of m^1A58 and O(6) of G18 (figure 2a,b). Thus, both cis-$[Pt(NH_3)(H_2O)]^{2+}$ binding sites are on N(7) of guanine bases.

$Ru(NH_3)_5$-tRNA Complex

Ruphe(25) shows two binding sites on tRNA for pentaammine ruthenium(III) (Table IV). Site 1 is located in the deep groove of the amino acid stem (figure 3). There is no direct coordination of the ruthenium to the tRNA bases at this site, rather the $[Ru(NH_3)(H_2O)]^{3+}$ complex ion is hydrogen bonded through ammonia ligands to the G4-U69 base pair and the adjacent bases in the helix, G3 and U68. The complex is stabilized by hydrogen bonds to both N(7) and O(6) atoms of the stacked guanines G3 and G4 and the O(4) keto

TABLE III.

a. cis-Pt Binding Sites

Site	Peak Height	Coordinates	Ligands (closest atoms)	Distance
Pt-1 (G15)	6.8σ	-0.32, 0.18, 0.26	G15 N(7)	2.08Å
			G15 O(6)	3.34
			O1P (15)	4.38
			O4 U(8)	4.01
			A14 N(7)	4.60
Pt-2 (G18)	5.6σ		G18 N(7)	2.32
			G18 O(6)	3.74
			m^1A58 N(6)	4.13

b. trans-Pt Binding Sites

Site	Peak Height	Coordinates	Ligands (closest atom)	Distance
Pt-1 (A73)	6.9	-0.05, 0.4, 0.12	A73 N(1)	1.29Å
			C74)(2)	3.64
			C74 N(3)	3.59
			G1 O(6)	4.11
Pt-2 (G^m34)	5.3	0.0, 0.15, 0.0	G^m34 N(7)	2.60
			G^m34 (O2P)	3.86
			G^m34 O(6)	4.24
Pt-3 (G43)	4.1σ	-0.25, 0.175, 0.13	G43 N(7)	2.30
			G43 (O1P)	3.94
			A44 (O1P)	3.79
			A44 N(7)	3.51
Pt-4 (G18)	3.90σ	0.1, 0.025, 0.31	G18 N(7)	1.27
			G18 O(6)	3.94
			G18 (O2P)	5.12
			m^1A58 N(6)	4.62

oxygen atoms of both stacked uracil bases (U68 and U69) on the opposite strand of the helix. The electrostatic binding mode observed here is analogous to that found for the binding of the inert $[Co(NH_3)_6]^{3+}$ ion in the monoclinic crystals of $tRNA^{phe}$ (18). However, no further analogy in the binding specificities of the Co and Ru complex ions is observed. At site 2 ruthenium is covalently bound to the N(7) atom of G15 in the dihydrouridine

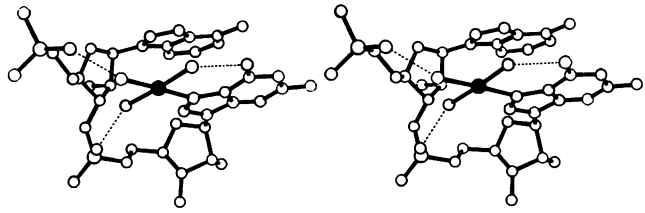

Figure 1. A stereoscopic view of the cis-Pt binding site at G15. Cis-Pt (solid ball) is directly coordinated to N(7) of G15 and forms interligand hydrogen bonds (dashed lines) to O(6) of G15 and phosphate oxygens on P15 and P14. $tRNA^{phe}$ coordinates are from ref. 16.

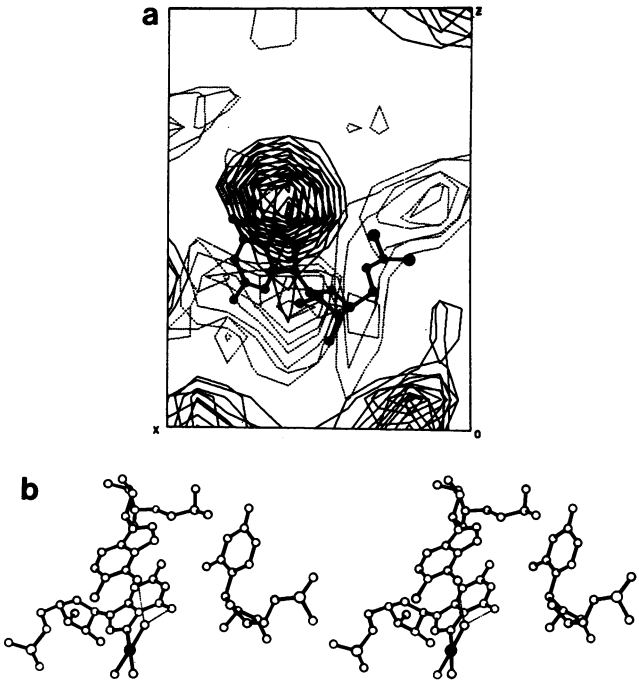

Figure 2a. A composite of the cis-Pt difference electron density map made up of six consecutive sections at 1.4Å intervals from the 5.5Å resolution map in the region around residue G18. The lowest contours are at 1.5 times the S.D. of the map with contour intervals of 0.5σ. The large peak of positive density corresponds to cis-$[Pt(NH_3)_2(H_2O)]$ bound to N(7) of G18. The skeletal model of G18 is shown superimposed on the electron density.
Figure 2b. A stereo plot of the cis-Pt binding site at G18. Cis-Pt (dark ball) is directly coordinated to N(7) of G18 and forms interligand hydrogen bonds (dashed lines) to O(6) of G18 and N(6) of m^1A58.

TABLE IV. Ruthenium Binding Sites

(a) Ruphe(25)

Ligand	Location and Coordinating atoms	Distance	Peak Heights/ Fractional Coordinates
	AA-Stem		
Ru(1)	N(7)(G3)	4.35	5.24σ/(-0.35,0.45,0.35)
	O(6)(G3)	3.85	
	N(7)(G4)	5.29	
	O(6)(G4)	4.09	
	O(4)(U68)	4.50	
	O(4)(U69)	3.96	
	D-Loop		
Ru(2)	N(7)(G15)	2.09	4.93σ/(-0.38,0.19,0.27)
	O(6)(G15)	3.54	
	O(1P)(G15)	4.24	
	O(1P(A14)	3.44	

(b) Ruphe(58)

Ligand	Location and Coordinating atoms	Distance	Peak Heights/ Fractional Coordinates
	D-Loop		
Ru(2)	N(7)(G15)	2.09	5.69σ/(-0.38,0.19,0.27)
	O(6)(G15)	3.54	
	O(1P)(G15)	4.24	
	O(1P)(A14)	3.44	
	AA-Stem		
Ru(3)	N(7)(G1)	2.02	4.98σ/(0.09,0.43,0.13)
	O(1P)(G1)	3.85	
	O(2P)(G1)	4.34	
	O(6)(G1)	3.70	
	D-Loop		
Ru(4)	N(7)(G18)	2.09	4.98σ/(0.12,0.03,0.32)
	O(6)(G18)	3.44	

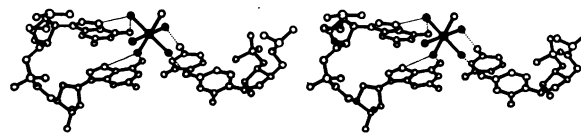

Figure 3. A stereo view of the $[Ru(NH_3)_5H_2O]^{3+}$ binding site to the G4-U69 wobble pair in the deep groove of the amino acid acceptor double helical stem observed in crystal Ruphe(25). The octahedral complex is hydrogen bonded through ammine groups to N(7) and O(6) of G3 and G4 and to O(4) of residues U68 and U69 as indicated by dashed lines.

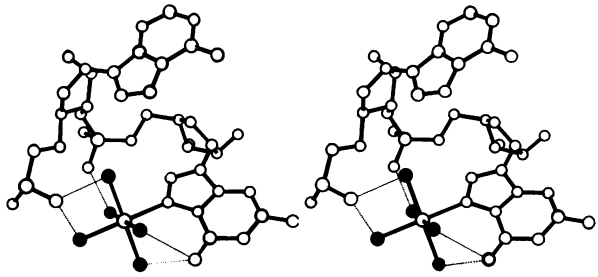

Figure 4. A stereo view of the bonding environment around the pentaammine-ruthenium binding site at residue G15. Ruthenium is directly coordinated to the N(7) position of G15 and is hydrogen bonded through the ammonia ligands to phosphate oxygen atoms of P14 and P15 and to O(6) of G15.

loop (figure 4). This binding apparently results in a significant shift of the G15 base (figure 5) suggesting possible disruption of the G15-C48 tertiary base pair. The complex is stabilized by hydrogen bonds between ammonia ligands and the keto oxygen O(6) of G15, and phosphate oxygens on P14 and P15 in a manner similar to the cis-Pt complex at N(7) of G15 described above.

The more extensively soaked crystal (Ruphe58) shows three ruthenium binding sites (Table IV). It is interesting that the deep groove binding site at the G4-U69 pair observed in Ruphe25 is no longer found. The binding of ruthenium to N(7) of G15 is observed with shifts in the position of the base similar to those discussed above. In addition to the G15 site, ruthenium is also found to be directly bound to the N(7) positions of residues G1 (figure 6) and G18 (figure 7a,b). The direct coordination to N(7) of guanine is characteristically stabilized by interligand hydrogen bonding between ammonia ligands on ruthenium and the O(6) keto oxygen of the guanine base. This interligand hydrogen bonding appears to confer in part the specificity of $[Ru(NH_3)_5]^{3+}$ binding to guanine bases.

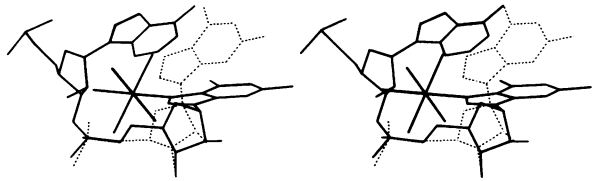

Figure 5. A stereo line drawing showing the proposed shift in the position of the nucleoside portion of residue G15 from the native $tRNA^{phe}$ structure (dashed lines) to that in the Ruphe(58) structure (solid lines).

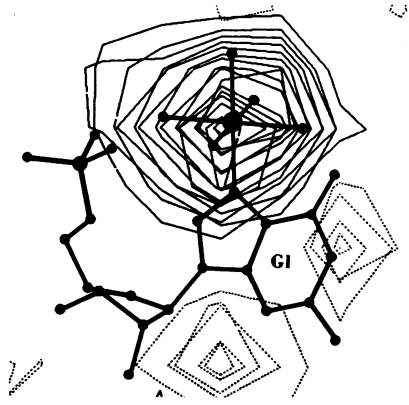

Figure 6. A composite difference electron density map of six consecutive sections (1.4Å intervals) for Ruphe(58). The contours start at ± 1.5σ and are at intervals of 0.5σ. Dashed lines represent negative contours. The N(7) binding of the $[(NH_3)_3Ru]^{3+}$ complex at G1 is shown superimposed on the electron density. Ruthenium (dark ball) is coordinated to N(7) of G1 and is hydrogen bonded through the ammonia ligands to O(6) of G1 and phosphate oxygens of the 5' terminal phosphate group.

Trans-Pt-tRNA Complex

The binding of trans-Pt to tRNA is in contrast to that of cis-Pt and $[Ru(NH_3)_5]^{3+}$. Crystals soaked extensively (23 days) in saturated trans-Pt solution show a single major binding site at the N(1) position of residue A73 in the acceptor stem. This complex is further stabilized by interligand hydrogen bonding to N(3) and O(4) of C74 and O(6) of G1 on the opposite RNA strand (figure 8a,b). A second trans-Pt is directly coordinated to N(7) of Gm34 in the anticodon loop. Interligand hydrogen bonds to O(6) of the base and a phosphate oxygen of P34 stabilize the complex. Two additional minor trans-Pt binding sites are observed. Both involve binding to the N(7) position of guanine bases; one binds to G18, as found for cis-Pt and Ru, and the other binds to G43. The G43 binding site is located at one end of the $tRNA^{phe}$ anticodon stem and is the only observed platinum binding site that is at a Watson-Crick base pair.

DISCUSSION

In previous studies cis-Pt was not found to bind in either orthorhombic or monoclinic crystals of $tRNA^{phe}$ (19-21). In fact, our present studies show no evidence of cis-Pt $tRNA^{phe}$ complex formation after four days of soaking, however soaking for a longer period (10 days) produced the cis-Pt·tRNA

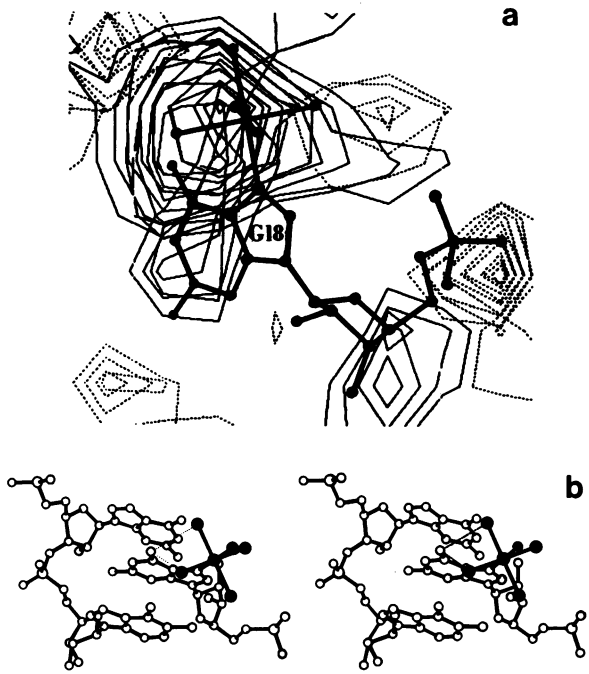

Figure 7a. The 5.5Å difference electron density showing Ru binding to N(7) of G18. Note suggested movements in some of the surrounding tRNA groups.
Figure 7b. A stereo plot showing the $[(NH_3)_5Ru]^{3+}$ binding site at G18. Ruthenium (dark ball) is coordinated to N(7) of G18 and forms interligand hydrogen bonds to O(6) of G18 through coordinated ammines. The $[(NH_3)_5Ru\text{-}G18]$ complex is shown intercalated between the bases of residues G57 and m^1A58. G18 is shifted slightly from its position in the native $tRNA^{phe}$ structure.

complex. The slow rate of reaction of cis-Pt is due to the presence of an excess of Cl^- ions in the tRNA crystals. This limits the rate of hydrolysis of cis-$[Pt(NH_3)_2Cl_2]$ to form cis-$[Pt(NH_3)_2(H_2O)_2]^{2+}$ which is believed to be the reactive species (22,23). Apparently the hydrolysis of trans-Pt occurs more rapidly under these conditions.

Cis-Pt binds strongly at two sites in orthorhombic crystals of $tRNA^{phe}$, viz., G15 and G18. In both cases direct coordination to the N(7) position of guanine is observed. The Pt coordination to guanine is monodentate. The previously proposed bidentate coordination to N(7) and O(6) (4) is not observed. The Pt-guanine complexes are stabilized by interligand hydrogen bonding to O(6) of the base. The guanines, G15 and G18 are both located in tertiary base paired regions of the molecule and neither is involved in

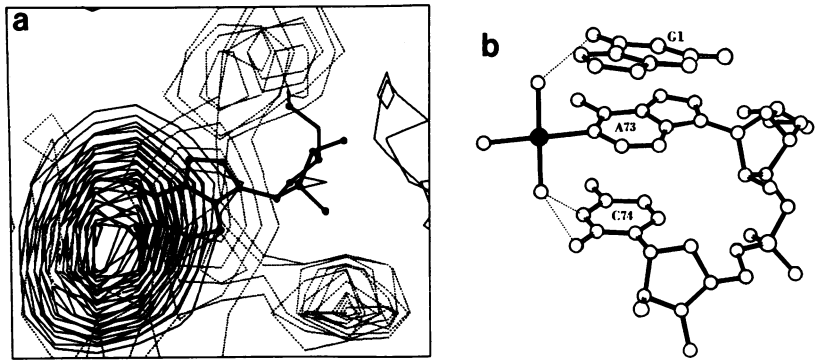

Figure 8a. A composite of the 5.5Å difference electron density map for trans-Pt made up of eight consecutive sections at 1.4Å intervals around residue A73. The large peak of positive density corresponds to trans-$[Pt(NH_3)_2 H_2O]$ bound to N(1) of A73. The skeletal model of A73 is superimposed on the map. Contour intervals are the same as in figure 2a.
Figure 8b. A plot of the trans-Pt binding site at A73. Trans-Pt (dark ball) is directly coordinated to N(1) of A73 and forms interligand hydrogen bonds to O(6) of G1 and N(3) and O(2) of C74.

standard Watson-Crick base pairing. Cis-Pt does not form intrastrand cross-links between adjacent guanines in $tRNA^{phe}$ although there are three regions in the molecule, G3-G4, G18-G19-G20, and G42-G43, which contain consecutive guanine sequences.

In contrast to cis-Pt, which shows a preference for the N(7) site of guanines, trans-Pt shows a preference for the N(1) site of adenine (A73). Relatively weaker binding to the N(7) positions of guanines G18, G^m34 and G43 is also observed. Although the binding site at G18 is common to both cis- and trans-Pt, binding at G^m34 and G43 is unique to trans-Pt. In monoclinic crystals of $tRNA^{phe}$ trans-Pt showed a single binding site at G^m34, however no binding to A73, G18 or G43 was observed (19,21). The minor trans-Pt binding site at G43 is the only instance observed for platinum binding in a double helix, although it should be noted that G43 is located at the terminus of the helical stem.

Pentaammine ruthenium(III) cations bind to the $tRNA^{phe}$ molecule at the N(7) sites of guanines, G1, G15 and G18, which are located at the ends of helical stems or in tertiary base paired regions of the $tRNA^{phe}$ molecule (figure 9). The binding of the octahedrally coordinated ruthenium cation to N(7) of G15 and G18 is similar to that observed for the square planar cis-$[Pt(NH_3)_2Cl_2]$ complex. The rotation of the square planar Pt group from the base plane allows this complex to interact with neighboring atoms in a manner

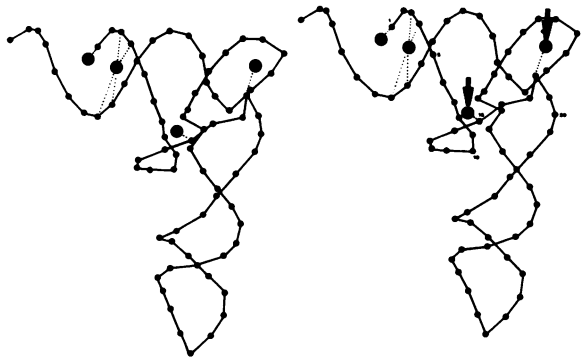

Figure 9. A stereo plot showing the $tRNA^{phe}$ phosphate backbone and positions of the four pentaammine-ruthenium binding sites on the molecule. Sites (G15 and G18) indicated by arrows are common to both Ru and cis-Pt.

similar to the octahedral Ru complex (see also below). The similarity in binding properties of these two metal complexes may underlie their carcinostatic properties. Both ruthenium and cis-platinum are observed to bind to the N(7) sites of specific guanines in non-helical regions of the tRNA molecule. Binding to these particular bases in $tRNA^{phe}$ is related to the fact that they are exposed and occur in a region of the molecule where the negative charge density of the phosphate groups is high (24). The same region of the molecule was previously observed to bind the aromatic cationic drug ethidium (25). Theoretical studies (26) have also shown that the highest negative charge density in the $tRNA^{phe}$ molecule resides in this region, consistent with the results of our binding studies. The specificity of binding of these carcinostatic drugs for guanine bases is in part determined by interligand hydrogen bonding between the ammonia ligands on the metal and the O(6) keto oxygen of guanine.

Although the present study was done on tRNA the results may provide information on the interaction of the complexes with DNA and the mechanism of action of these metal complexes. It appears that both the cis-Pt and ruthenium complex ions show a reluctance to bind to bases in the Watson-Crick base paired double helical stems. The binding of ruthenium to the 5' terminal base of the acceptor stem helix (G1) is an exception. Binding at this site seems to be correlated with the non-covalent binding to the G4-U69 "wobble" base pair. Thus binding within the deep groove of the helix and to the proximal G1-C72 base pair are mutually exclusive. Model studies of cis-Pt complexes of nucleosides (6,9-10) indicate that the square planar platinum

complex is twisted at an angle of about 90° to the base plane. The twist alleviates the steric clash between the Pt-ligand and the guanine keto oxygen atom O(6) and is usually accompanied by an interligand hydrogen bond between a Pt-ligand and the O(6) atom. In this preferred twisted coordination geometry, it is seen that binding to N(7) in the deep groove of the double helix would produce unfavorable Van der Waals contacts between the Pt ligands and the base stacked on the 5' side. Thus, the failure of these drugs to bind covalently in the helical stems is probably a consequence of the decreased exposure of the guanine N(7) sites in the deep groove of the RNA double helix.

Several features of the observed binding of these drugs to tRNA may have broader implications in our efforts to understand their interactions with DNA. B-DNA is more extended than RNA or A-DNA, and although the N(7) atom of the guanine is more exposed in the major groove the 5'-side base is still expected to cause some obstruction to binding to the N(7) site. In fact, recent results on the crystal structure of a cis-platinum - DNA dodecanucleotide complex (ref (28) and R. Dickerson, private communication) gave similar results to our tRNA studies, vide infra specific Pt binding to the N(7) sites of guanine with monodentate coordination. The steric problem which we have presented above seems to explain the weak binding (low occupancy) of cis-Pt to the B-DNA double helix.

It would appear that strong binding (high occupancy) of the Pt drug to B-DNA will necessitate distortion of the double helix or even possible local denaturation. However, in the left-handed Z-DNA it can be seen that the guanine N(7) site is even more exposed. This arises from the fact that only the interleaving G-C base pairs are twisted with respect to each other, since adjacent base pairs are stacked with zero twist angle, and thus the steric conflict between the metal complexes and the 5'-stacked base is minimized. From the above steric considerations it would be expected that regions of Z-DNA, locally distorted regions of B-DNA, or single stranded regions of DNA will preferentially bind the carcinostatic metal complexes. Recent solution studies corroborate our theory. Cis-Pt is found to bind to both B- and Z-DNA. Circular dichoric spectra of the cis-Pt complex with B-DNA indicates that a unique DNA conformation is formed upon complexation (29). Thus, the binding of the cis-Pt to the B-form of DNA is accompanied by significant changes in the DNA conformation as we have envisaged above. In contrast, the binding of cis-Pt to Z-DNA does not induce such conformation changes since the guanine N(7) sites in Z-DNA are readily accessible. Furthermore, the

binding of cis-Pt stabilizes the Z-DNA structure (M. Leng, private communication). The induced conformational changes in B-DNA, or the stabilization of the Z-DNA structure by cis-Pt may be responsible for the carcinostatic properties of this drug.

ACKNOWLEDGMENTS

We gratefully acknowledge the National Institutes of Health for supporting this project through grants GM-18455 and GM-17378. Continued support from the College of Agricultural and Life Sciences of the University is also acknowledged.

Present address: Laboratory of Stereochemistry, National Research Council, Via F.D. Guerrazzi, 27, 50132 Florence, Italy.

*To whom correspondence should be addressed.

REFERENCES

1. a. Rosenberg, B., Van Camp, L., Trosko, J. E. and Mansour, V. H. (1969) Nature (London) 222, 385-386. b. Rosenberg, B. (1980) in Nucleic Acid-Metal Ion Interactions, Spiro, T. G., Ed., pp. 1-29, J. Wiley & Sons, New York.
2. Roberts, J. J. and Thomson, A. J. (1979) Prog. Nucl. Acid Res. Mol. Biol. 22, 71-133.
3. Stone, P. J., Kelman, A. D. and Sinex, F. M. (1974) Nature (London), 251, 736-737.
4. Rosenberg, B. (1978) Biochimie 60, 859-867.
5. Kelman, A. D. and Buchbinder, M. Biochimie (1978) 60, 893-899.
6. Marzilli, L. G. (1977) Prog. Inorg. Chem. 23, 355-378.
7. Goodgame, D.M.L., Jeeves, I., Phillips, F. L. and Skapski, (1975) Biochem. Biophys. Acta 378, 153-157.
8. Gellert, R. W. and Bau, R. (1975) J. Am. Chem. Soc. 97, 7379-7380.
9. Kistenmacher, T. J., Chiang, C. C., Chalilpoyil, P. and Marzilli, I. G. (1979) J. Am. Chem. Soc. 101, 1143-1148.
10. Cramer, R. E. and Dahlstrom, P. L. (1977) J. Clin. Hematol. Oncol. 7, 330-337.
11. Kelman, A. D., Clarke, M. J., Edmonds, S. D. and Peresie, H. J. (1977) in Proceedings of the Third International Symposium on Platinum Coordination Complexes in Cancer Chemotherapy, Wadley Institute of Molecular Medicine, p. 1, 274-288.
12. Clarke, M. J. (1980) in Inorganic Chemistry in Biology and Medicine, ACS Symp. Series 140, 157-180.
13. Munchausen, L. and Rahn, R. A. (1975) Biochim. Biophys. Acta 412, 242-255.
14. Vogt, L. H., Katz, J. L. and Wiberly, S. E. (1965) Inorg. Chem. 4, 1157-1163.
15. Rubin, J. R., Wang, J. H. and Sundaralingam, M. (1983) Biochim. Biophys. Acta 756, 111-118.
16. Sussman, J. L. and Kim, S. H. (1976) Biochem. Biophys. Res. Commun. 68, 89-96.
17a. Wu, S. M. and Bau, R. (1979) Biochem. Biophys. Res. Commun. 88, 1435-1442.

17b. Kastner, M. E., Coffey, K. F., Clarke, M. J., Edmonds, S. E. and Eriks, K. (1981) J. Am. Chem. Soc. 103, 5747-5752.
18. Hingerty, B. E., Brown, R. S. and Klug, A. (1983) Biochim. Biophys. Acta, 697, 78-82.
19. Stout, C. D., Mizuno, H., Rao, S. T., Swaminathan, P., Rubin, J., Brennan, T. and Sundaralingam, M. (1978) Acta Cryst. B34, 1529-1544.
20. Teeter, M. M., Quigley, G. J. and Rich, A. (1980) in Nucleic Acid-Metal Ion Interactions, Spiro, T. G., Ed., pp. 146-177, John Wiley & Sons, New York.
21. Jack, A., Ladner, J. E., Rhodes, D., Brown, R. S. and Klug, A. (1977) J. Mol. Biol. 111, 315-328.
22. Mansy, S., Chu, G. Y. H., Duncan, R. E. and Tobias, R. S. (1978) J. Am. Chem. Soc. 100, 607-616.
23. Mansy, S., Rosenberg, B. and Thomson, A. J. (1973) J. Am. Chem. Soc. 95, 1633-1640.
24. Sundaralingam, M. (1981) in Proceedings of the International Symposium on Biomolecular Structure, Conformation, Function and Evolution, Madras, January 1978, Vol. 1. Diffraction and Related Studies, Srinivasan, R., Subramanian, E. and Yathindra, N., Eds. pp. 259-283, Pergamon Press, Oxford.
25. Liebman, M., Rubin, J. and Sundaralingam, M. (1977) Proc. Natl. Acad. Sci. USA, 74, 4821-4825.
26. Lavery, R., Pullman, A. and Corbin, S. (1981) in Proceedings of the Second SUNY Conversation in the Discipline Biomolecular Stereodynamics, Sarma, R. H., Ed., Vol. 1, pp. 185-193, Adenine Press, New York.
27. Rubin, J. R., Sabat, M. and Sundaralingam, M. (1983) in Nucleic Acids - The Vectors of Life (1983) (B. Pullman and J. Jorkner, Eds.) in press.
28. Wing, R., Drew, H., Takano, T., Broka, C., Tanaka, S., Itakura, K. and Dickerson, R. E. (1980) Nature (London), 287, 755-758.
29. Malfoy, B., Hartmann, B. and Leng, M. (1981) Nucleic Acids Res., 9, 5659-5669.